ORIGINAL PAPER

Identifying the contribution of rotational movement in pottery forming based on statistical surface analysis

Richard Thér[1] · Josef Wilczek[2]

Abstract

This article explores the possibilities of distinguishing different pottery forming methods utilising rotational movement based on a statistical analysis of the surface topography and variations in wall thickness. The presented topographic analysis is based on calculation of the surface regularity that is approached as measurement of the difference between the 3D representation of the pottery surface and the corresponding ideal vessel shape, obtained by rotating a model profile around the rotational axis. These differences are expressed using basic surface roughness parameters. In addition, analysis of wall thickness variability and the overall shape of the horizontal sections using elliptic Fourier analysis (EFA) were performed. The study was based on a pilot experimental dataset of vessels made using three forming methods: coiling in combination with wheel finishing employed using a turntable and using a potter's wheel and wheel throwing. The results show that, with an increasing contribution of rotational movement in the forming sequence, a gradual increase in the regularity of vessel shapes and a decrease in wall thickness variability are observed. The differences in these two parameters allow us to distinguish among the studied forming methods. Automatic classification using elliptic Fourier analysis and support vector machine (SVM) indicates reliable classification for the lower parts of the experimental vessels.

Keywords Wheel throwing · Pottery forming · Topographic analysis · Surface roughness · Elliptic Fourier analysis · Automatic classification

Introduction

Pottery forming methods represent a valuable source of information, not only on the diversity and development of the manufacturing processes themselves, but also for addressing the broader issues related to the social networks to which the potters were subject (e.g., Derenne et al. 2020; Gallay 2012; Gelbert 2003; Gomart et al. 2017; Gosselain 1998, 2000, 2002, 2008; Mayor 2010; Roux 2011, 2017, 2019; Roux et al. 2017). However, applying the results to studying forming techniques to better understand past societies depends on our ability to reliably identify these techniques in sufficient detail on a statistically representative proportion of the studied ceramics.

Forming is one of the basic steps in pottery manufacturing. Procedures employed in forming are based on movement of the hands and other tools (e.g. potter's blades, spatulas, paddles and anvils, potter's wheel), causing plastic deformation of the clay (e.g., Rice 2015; Roux 2019; Rye 1981). The way the clay is formed produces specific phenomena related to the inner structure of the components of the clay body and topography and morphology of the object surface. Therefore, there are two essential sources of evidence for pottery forming techniques: inner structure and surface morphology and topography (Thér 2020 and references therein). This article is focused on the surface topography. The advantage of surface analysis is that the surface is accessible to the naked eye. Consequently, data acquisition for the analysis is less demanding than analysis of the internal structure of the object. On the other hand, the surface topography is transformed in later stages of forming (especially by finishing and surface treatment techniques), which usually obliterates the features resulting from previous forming stages.

✉ Richard Thér
   richard.ther@uhk.cz

[1] Department of Archaeology, Philosophical Faculty,
    University of Hradec Králové, Rokitanského 62,
    CZ-50003 Hradec Kralove, Czech Republic

[2] Centre André Chastel/UFR Histoire d'art et Archéologie,
    Faculty of Arts and Humanities, Sorbonne University, 1 rue
    Victor Cousin, FR-75005 Paris, France

The most common method of analysis of surface residues of pottery forming is visual observation and description of the observed phenomena (e.g. Choleva 2012; Doherty 2015; Dupont-Delaleuf 2011; Gomart 2011, 2014; Jeffra 2013; Knappett 1999; Kudelić 2020; Martineau 2002; Méry et al. 2012; Rosselló and Trias 2013; Roux 2019; Rückl and Jacobs 2016; van Doosselaere 2010). The observations related to pottery forming are most commonly classified or described in the given set of qualitative categories. The advantage of the qualitative approach is that complex phenomena can be captured using a suitable set of categories. The qualitative macro-trace classification approach relies on a well-developed methodology with established terminology and analytical protocol (see especially Roux 2019 for the comprehensive synthesis of the current state of research). However, in practice, it may face problems related to the fact that naked eye observation–based classification (regardless of whether the eye observes the original sample or its visual representation, e.g. 3D scan) depends on the abilities and experience of the researcher. Such classifications may not be reproducible until quantified (e.g., Hodson et al. 1966; Wilczek et al. 2014). However, we are not proposing the substitution of the traditional qualitative approach for the quantitative one. In many cases, quantification reduces the complexity of diagnostic features to only a few aspects that can be measured. We perceive it as a complement to the methodological mosaic of a comprehensive approach to studying pottery-forming techniques. It is helpful to focus the quantitative analysis only on specific topographical characteristics. This article explores one of them — surface regularity as an effect of the pottery forming method.

So far, the quantitative approach has not been widely employed in the field of pottery-forming analysis. Quantitative analysis has been applied to surface topography, roughness and microscopic traces to some extent since the 1980s and has been more common since 2000, with studies concerned with measuring the tribological interaction between the surface of the tool and that of the worked lithic, bone or shell material (see Evans et al. 2014 for the general overview; see Stemp 2014; Stemp et al. 2015b for a very detailed review and history of lithic microwear studies from the nineteenth century onwards). A typical microwear (use-wear) study aims to distinguish between tools of a given material (e.g. chert, flint, obsidian), actions (e.g. sawing, notching, scraping) and duration (e.g. the number of strokes) on different contact materials (e.g. wood, wheat, shell, antler, hide, meat, pottery). Data for analysis (e.g. profiles, images and/or 3D models) are usually acquired using a laser profilometer (e.g., Stemp et al. 2009; Stemp and Stemp 2001), laser scanning confocal microscope (LSCM; e.g., Evans and Donahue 2008; Evans and Macdonald 2011; Macdonald and Evans 2014), atomic force microscopy (AFM; e.g. Kimball et al. 1995; Faulks et al. 2011; Laskaris et al. 2017) or variable

focus microscopy (FVM; Macdonald 2014a, see also Stemp et al. 2015b).

This study represents one of the first attempts to employ quantitative topographical analysis to identify specific aspects of pottery forming. It focuses on a particular phenomenon related to pottery forming: the use of rotation movement and its relation to vessel surface regularity and wall thickness uniformity. The fundamental question underlying the research is whether it is possible to reliably differentiate among the different contributions of rotational movement in the forming sequence based on quantitative surface analysis. The analysis is performed on a pilot experimental dataset representing a vessel replicated using three forming methods utilising rotational movement. Consequently, the results are strictly related to these technological phenomena. Their application to other forming methods must be based on specific hypotheses derived from the theoretical relationship between the forming methods and the surface topography.

The benefit of this approach for archaeology is that it provides quantitative results using fast and cost-effective acquisition of analytical data without any destructive impact on the archaeological samples. To estimate the applicability to archaeological pottery, which is in most cases fragmented, we performed the analysis not only on the whole experimental vessels but also on segments of these vessels simulating the fragmentary state of the artefacts.

Theoretical relation of surface topography, variation in wall thickness and forming methods

Topography perceives the surface as a continuum and describes surface relief mainly based on quantitative dimensional measurements (O'Connor et al. 2003; Sahoo 2011). The principle of topographical analysis is based on the idea that the actual relief contains irregularities, and these irregularities are measured as deviations from defined reference surfaces (Whitehouse 2002). In the context of analysis of pottery-forming techniques, these deviations are a potential source of evidence for the employed forming techniques. The techniques used in the initial forming of the primary vessel shape cause a characteristic surface topography, reflecting the form of the segments from which the vessel is assembled and movements used while joining and transforming the segments into a raw vessel shape. The potters might intend to leave these features untransformed as decorative or functional elements. However, in most cases, this vessel form is considered unsatisfactory in terms of the function (e.g. the segments are not connected strongly enough), or the aesthetical appearance (uneven raw surface) and shaping continue towards the desired appearance. The potters stop shaping

when they evaluate that the shape has adequate aesthetic or functional properties or reach the limits of their skills.

Therefore, the deviations from ideal geometry can be intentional (for some functional or aesthetic reasons) or unintentional (caused by negligence, lack of skills or lack of motivation to achieve the intended geometry). The unintentional deviations reflect the forming techniques and their mastering, and topographical analysis concerning forming aims to express the nature of these deviations. The starting point is the *materialised form* of the vessel, i.e. the final form that can be observed. The *ideal form* is a geometrical abstraction eliminating both the deviations mentioned above. However, it differs from the *intended form*. The intended form combines ideal form and intentional deviations that are usually related to surface modifications. The intended form eliminates only unintentional deviations and is close to the potter's mental concept of the form (Thér 2020). The difference between the materialised form and the intended form is of primary interest in analysing forming techniques.

Analysis of the variation in wall thickness provides additional information that cannot be extracted from a single surface. Wall thickness analysis enables the study of spatial relations between the external and internal surface topography of the vessel, as well as topography-independent variations in thickness. The local variation is closely related to the surface topography. Surface shapes and features are manifested by the variability in the wall thickness. Consequently, the study of local thickness variability constitutes topographical analysis based on 1D representations of the surface profiles. Study of variations

in the local wall thickness can be viewed as contextual topographical analysis of both surfaces: the exterior and interior.

In addition, the global variation in the wall thickness refers to the difference in wall thickness throughout the entire vessel. It reflects the forming history even when subsequent stages of manufacture entirely obliterated the topography caused by roughing out of the vessel.

Quantification of surface topography and variation in wall thickness

Surface regularity can be quantified on the basis of the distances measured between locations in a 3D representation of the materialised form of the vessel and the corresponding ideal vessel shape, obtained by rotating a model profile around the rotational axis. Since the late 1990s, several approaches have been proposed to identify the optimum position of the rotational axis of the vessel based on 3D models (e.g., Halíř 1999; Karasik and Smilansky 2008; Sablatnig et al. 2005; Wilczek et al. 2018). When simplified to 2D representation (section view), the distances can be measured between points on a vessel's actual section and its approximated ideal form. Since the analysis aims to detect unintentional deviations from the ideal shape, a horizontal section is optimum for the analysis. Potters usually intend to achieve a circular shape of the vessel in horizontal sections. Consequently, the deviations can be measured as the distances between points lying on a horizontal section of the vessel and an ideal circle passing
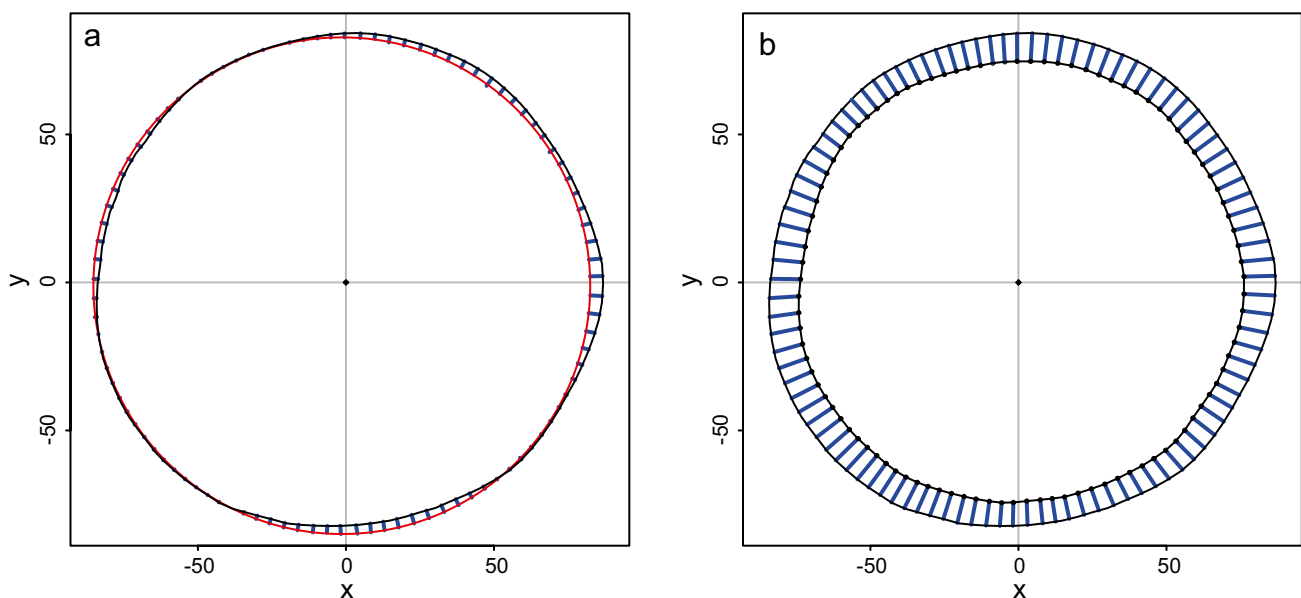

**Fig. 1** Extraction of parameters related to the surface. **a** Surface regularity. **b** Wall thickness

through these points (Fig. 1a). Note that if the ideal shape of the vessel in the horizontal section is not considered to be a regular circle, deviations from an ellipse or any other ideal shape approximating the vessel's surface can be used instead.

Another parameter that can be used in quantitative analysis is the *wall thickness*. This parameter can be calculated as the distance between a given point on one side and the projection along its normal on the other side of the surface (Fig. 1b).

Variations in these parameters are related to the surface roughness. Roughness can be understood as a geometric irregularity, a deviation of the materialised surface from the ideal form along the normal vector. Large deviations indicate an uneven surface, while slight deviations reflect a smoother surface. Much attention has been paid to the study of roughness in technical sciences as well as in archaeology. The metrics employed are generally univariate traditional linear and surface roughness parameters designated by international standards (ISO 25178 Surface Texture (ISO 2012)). These standards distinguish six categories of surface roughness parameters. The basic category, height parameters, quantifies any change in the surface within a particular zone of interest. The most common height parameters used in archaeology are the arithmetical mean height of surface (Sa; Evans and Donahue 2008), the root mean square height of the surface area (Sq; Evans and Macdonald 2011; Macdonald 2014a; Macdonald et al. 2018) and the root mean square height of surface profile (Rq; Stemp and Stemp 2003; Evans and Donahue 2008; Macdonald 2014b), which can sometimes be combined (Stemp and Stemp 2001; Werner 2018). Along with traditional roughness measurements, fractal geometry is also used in archaeology to determine the surface roughness (e.g., Brown et al. 2005; Moropoulou et al. 2007; Stemp et al. 2008; Stemp and Stemp 2001, 2003; Zorlu 2008). As the results obtained by employing the fractal dimension calculated from traditional roughness parameters (e.g. from Rq) are scale-dependent, the measurements of the relative length ($Rel\ L$; Stemp et al. 2010), relative area ($Rel\ A$; Zorlu 2008; Stemp 2014; Key et al. 2015) and area-scale fractal complexity ($Asfc$; Stemp et al. 2013, Stemp et al. 2015a) have been adopted by the archaeological community to quantify multiscale surface complexity.

Besides these techniques, it can also be expected that the *overall shape of the horizontal section* itself contains valuable information about the forming method. From this point of view, modern geometric morphometrics can be used to quantify and compare the shape of sections (e.g. Brande and Saragusti 1996; Buchanan and Collard 2010; Wilczek et al. 2014). As these sections are usually expressed as closed circular (or oval) outlines, elliptic Fourier analysis (Kuhl and Giardina 1982) seems to be a reasonable choice for the calculation of shape variables.

The quantitative approach places greater demands on the quality of the data obtained by the imaging methods. Searching for phenomena characteristic for pottery forming, the tools and techniques that can capture a wide area of a larger sample, or even the whole object (both sides of the vessel wall or the entire shape) in sufficient resolution are preferred. Stationary or handheld 3D scanners are suitable devices when the flexible acquisition of a 3D representation of a whole solid is required to investigate the topography at the macro- and mesoscopic scale or the variability in wall thickness (Karasik and Smilansky 2008; Revello Lami et al. 2016; Wilczek et al. 2018).

Application

This study employed these concepts to distinguish among different forming methods using rotational movement. We hypothesise that the different contributions of rotational movement to the whole forming sequence cause different deviations from the ideal form of the vessel. During throwing, potters exert continuous pressure. They may vary the pressure during forming (intentionally or unintentionally), but the usual way is to keep the pressure constant as much as possible. Given the rotation speed, the pressure changes cause gradual changes in thickness in the direction of the forming vector. This leads to a smooth profile with minimal deviation from circularity or ellipticity and even thickness in the plane parallel to the resulting vector of the force applied in deformation of the clay. However, the vector is not horizontal. Its direction results from the combination of upward-lifting by the fingers or other tools and rotation around the vertical axis. If the surface is not finished with the blade, the upward-lifting with the fingers leaves a diagonally oriented undulating relief in the vessel's interior (e.g. Roux 2019). A horizontal section obliquely cuts the undulated relief, resulting in a profile of long waves. This kind of geometry corresponds to specific regular deviations from the ideal form.

In the case of wheel throwing, all the topography is created on the potter's wheel by continuous pressure. When continuous pressure is applied to a roughout with topography defined by some other roughing-out technique, the continuous pressure transforms the initial topography. Perfection of this transformation depends on the contribution of rotational movement to the whole sequence, which can be expressed as the amount of work performed by continuous pressure (c.f., Henrickson 1991; Courty and Roux 1995; Roux and Courty 1998; Roux 2003; Berg 2007, 2008; Choleva 2012; Thér and Toms 2016; Thér 2016; Thér et al. 2017).

In our pilot study, we employed the analysis of a collection of three forming methods utilising rotational movement:

a. *Coiling combined with wheel finishing employed using a turntable* (*CTF*). The vessel is formed by coiling, and, subsequently, rotational movement is used for surface modifications and minor shape corrections. The fingers exert the pressure. The turntable produces a minimal amount of rotational energy that does not effectively employ continuous pressure. In addition, the fingers are soft and curved tools cause a loss of the energy needed to transform the surface. As a result, the transformation speed of the technique is low.

b. *Coiling combined with wheel finishing on a potter's wheel* (*CWF*). The vessel is formed by coiling, and subsequently, rotational movement is used for surface modifications and minor shape corrections. A potter's blade exerts the pressure. The potter's wheel produces a large amount of rotational energy, allowing effective use of continuous pressure. The hard and straight working edge of the blade secures effective transformation of energy to forming force. As a result, the transformation rate of the technique is significantly greater than in the previous case.

c. *Wheel throwing* (*WT*). The entire forming sequence was performed using rotational energy.

Dataset, data acquisition, section extraction and method of analysis

Dataset

The experimental dataset used for this pilot study was composed of 27 bowls manufactured by a professional potter (Fig. 2, SM1). Each bowl was approximately 10 cm high, with a maximum diameter of 23 cm. There are two basic reasons for the selection of the shape and dimensions of the replicated vessels: (a) a bowl is a common type of pottery found abundantly in many archaeological contexts in different geographical regions; (b) it represents a vessel shape requiring a moderate level of skills, thus allowing demonstration of differences in the execution of forming methods.

Complete vessels were analysed in the first phase of the analysis to avoid problems related to estimation of the precise position of the rotational axis. Three forming methods were used (i.e. *CTF*, *CWT*, *WT*), and 9 bowls were produced using each of them. All the experimental vessels were fabricated from commercial fine-grained clay (Pávek Keramika, product designation: točířská hlína ROT) and fired in an electric kiln to 800 °C under oxidising conditions.

Data acquisition

The workflow used for quantitative analysis can be briefly described as follows. All 27 vessels were scanned in 3D using an Artec Space Spider scanning device, with an accuracy of down to 0.05 mm and a 3D resolution of 0.1 mm (Fig. 2a; Artec 3D 2020), and processed in Artec Studio 15 (Artec 3D 2021). The 3D scan of each vessel was created by alignment, registration and fusion of several partial scans, each covering a different part of the vessel. Only those parts where alignment and registration values fell within the best class of the registration quality defined by the standards of the scanning device producer (<0.1 "good results"; Artec 3D 2021) were used for creation of the 3D model. The number of polygons acquired on each vessel varied between 40 and 50 million triangles. In the next step, each 3D model was manually oriented to align its base with the natural surface on which the artefact originally stood (Fig. 2b). Then, three horizontal planes were defined: at the level of the neck (noted NECK in the text), at the maximum body diameter (noted MAX), and at the lower part of the body (noted LOW; Fig. 2c). Each plane cut the outer and inner surfaces of the bowl, thus creating 6 horizontal sections per vessel. In order to standardise the number of points, each section was sampled by 1000 equally spaced points (Fig. 2d). Finally, the centres of circles corresponding to the rotational axis were calculated, based on the least-squares method (Fig. 2e; Chernov 2010).

To investigate the potential application of the method to fragmented archaeological pottery (representing only parts
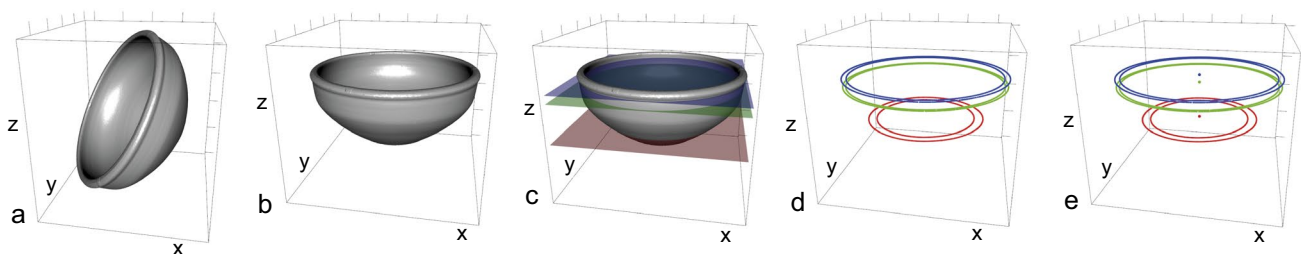
Fig. 2 Data acquisition and section extraction. **a** Non-oriented 3D model of the vessel. **b** 3D model oriented according to the rotational axis. **c** Three horizontal planes defined on the vessel, at the neck (blue plane), at the maximum body diameter (green plane) and at the lower part of the body (red plane). **d** Six sections (each composed of 1000 points) defined by the intersection of the outer and inner surfaces of the vessel and the three horizontal planes. **e** Extraction of centres of circles corresponding to the rotational axis

of the circumference of the vessel), each horizontal section was additionally segmented into 2, 4 or 8 fragments of equal size (i.e. two halves, four quarters and eight eighths). This segmentation, where each subsequent segment is half the previous one, was chosen to identify the limits of applicability of the method in relation to the fragmentation of archaeological material. Segment analysis was limited to the parameters and vessel parts that have proven most valuable in differentiating among forming methods.

Surface regularity

The first analysis was based on comparison of the vessel regularities, reflected in the distances between points on the section and a perfect circle passing through them. Several basic roughness parameters, such as the mean height (Ra), maximum height (Rz) and root mean square height (Rq), were then calculated from 162 sections.

Wall thickness

The second analysis was based on comparison of vessel thicknesses, calculated from the distances between points on the inner side of the vessels and their projections on the outer side. Three measurements (the mean distance, the range of the values and the standard deviation) were calculated for each section.

Discrimination using geometric morphometrics

Analysis based on geometric morphometrics is aimed at identifying which part of the vessel (i.e. neck, maximum body diameter, lower part) is most suitable for distinguishing among the three forming methods. The morphometric procedure was as follows: all the section outlines were oriented on the first principal component axis in the first step, and the starting point was set at the maximum x-coordinate point. Based on this point, 200 equidistant points were traced along the outline (Fig. 3a). These points were then treated by elliptic Fourier analysis (Kuhl and Giardina 1982), decomposing the outline into an infinite series of repeating trigonometric functions called harmonics. Each harmonic is composed of four Fourier coefficients (Fig. 3b). The greater the number of harmonics is, the better the reconstruction of the original contour. In order to take into account only the shape of each section and not its size or orientation, all the sections were normalised according to the major axis of the first harmonic and all coefficients were size-normalised using the square root of the harmonic amplitudes (Furuta et al. 1995; Rohlf and Archie 1984; Zhan and Wang 2012). As the values of the first harmonic became constant after this operation, they were omitted from further analysis.

The optimal number of harmonics was estimated by Harmonic power (Lestrel 1997). The number of harmonics representing at least 99% of the original shape of the sections was retained for further analysis.
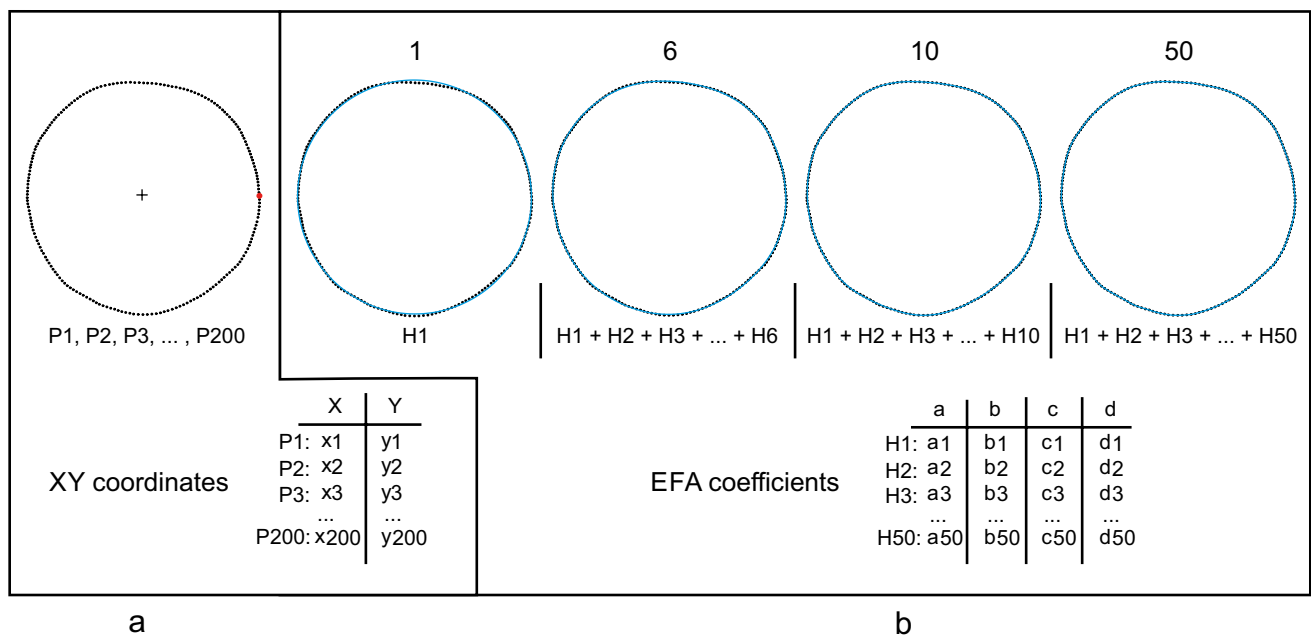
Fig. 3 Elliptic Fourier analysis. **a** The original Cartesian coordinates of the outline. The red dot corresponds to the first point on the outline. **b** The original Cartesian coordinates of the outline are decomposed into a set of harmonics. A given number of harmonics are used to reconstruct the approximation of the original contour (here 1, 6, 10 and 50 harmonics)

Discrimination between sections was performed using support vector machine (SVM, (Cortes and Vapnik 1995)). This machine-learning classification algorithm seeks to maximise the gap between different categories. This is carried out by maximising the distance between the decision boundary hyperplane and the support vectors, which are the samples located closest to this hyperplane. As the number of analysed sections was relatively small, a leave-one-out cross-validation strategy was selected for the classification validation. Because the SVM uses several parameters that are randomly initialised, multiple SVM calculations (here 1000) were performed to ensure the robustness of the results.

Results

Surface regularity

The distribution of the basic roughness parameters (*Ra*, *Rz* and *Rq*) for the three forming methods can be seen in Fig. 4. All three parameters express similar tendencies. The distribution of the standard deviations indicates that the least regular (deviating most from the ideal form) vessels are formed by *coiling with turntable finishing* (*CTF*), followed by *coiling with potter's wheel finishing* (*CWF*), while the *wheel-thrown* (*WT*) vessels are the most regular. Each group appears to be very different from the others — there is no significant overlap between them. The differences between the groups were also confirmed by the Kruskal-Wallis rank sum test (Table 1), followed by Wilcoxon rank sum post hoc tests (Table 2).

Interestingly, in all cases, maximum height values never exceeded 6 mm (Fig. 4: *Rz*). Therefore, it seems that, with all three methods, the potter succeeded in forming shapes with high regularity: even vessels formed by *CTF* may be

Table 1 Vessel surface regularity. Kruskal-Wallis rank sum test

	KW test	Df	p
Ra	96.848	2	< 2.2e−16
Rz	105.92	2	< 2.2e−16
Rq	98.908	2	< 2.2e−16

considered symmetrical, while the *WT* vessels appear almost perfectly identical.

The distribution of *Rq* values calculated for the combination of section position and type of forming technique reveals that each forming technique seems to be clearly differentiable based on the vessel section position (Fig. 5; Table 3). The most different are sections from the lower parts of the vessels, followed by sections taken at the maximum diameter of the vessels. The neck section appears to differentiate only between vessels formed using *CTF* and *WT* methods.

The graph depicting the distributions of the *Rq* values ordered according to forming technique shows that vessel regularity decreases slightly from the bottom to the upper part of the vessel for the CWF and WT techniques (Fig. 6). The lower parts of the CTF are less regular and statistically different from the sections of the other two positions (see Table 3).

The analysis of segments of decreasing arc length (i.e. halves, quarters and eighths) was performed in the position that exhibited the greatest potential for forming method discrimination, i.e. the lower parts of the vessels. The differences between forming techniques decrease as the size of the fragments decreases (Fig. 7). Similar tendencies were nevertheless observed. There is only a slight overlap between forming techniques, and the differences are statistically significant (Tables 4 and 5).
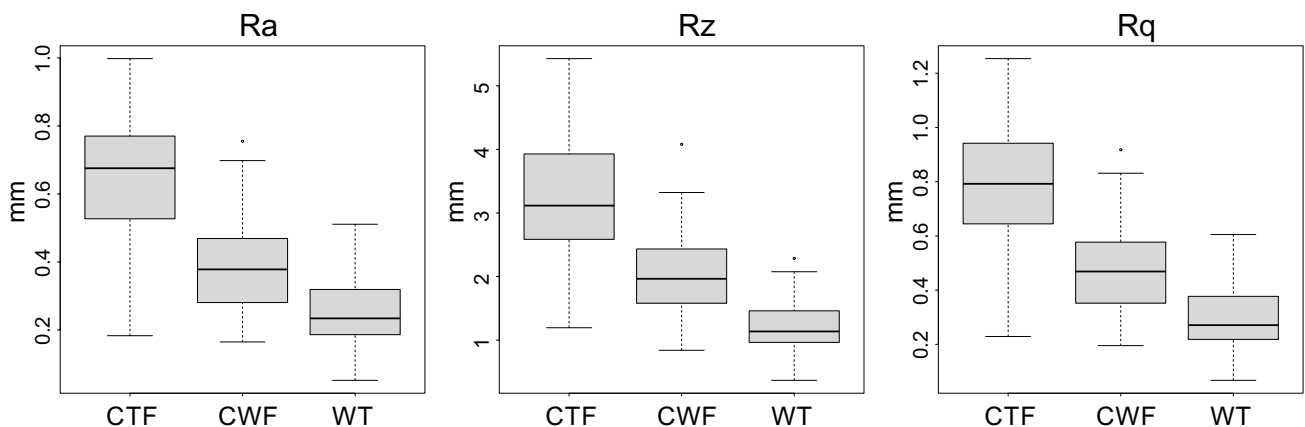
Fig. 4 Vessel regularity. 162 sections (i.e. 27 vessels × 6 sections). Distribution of roughness parameters according to the forming method. *Ra*, mean height; *Rz*, maximum height; *Rq*, root mean square height

Table 2 Vessel surface regularity. Post hoc pairwise comparison using the Wilcoxon rank sum test with the Bonferroni correction

Ra	CTF	CWF	WT
CTF	-		
CWF	4.3e-11	-	
WT	< 2e-16	2.8e-08	-

Rz	CTF	CWF	WT
CTF	-		
CWF	6.2e-10	-	
WT	< 2e-16	4.5e-12	-

Rq	CTF	CWF	WT
CTF	-		
CWF	7.7e-11	-	
WT	< 2e-16	4.7e-09	-
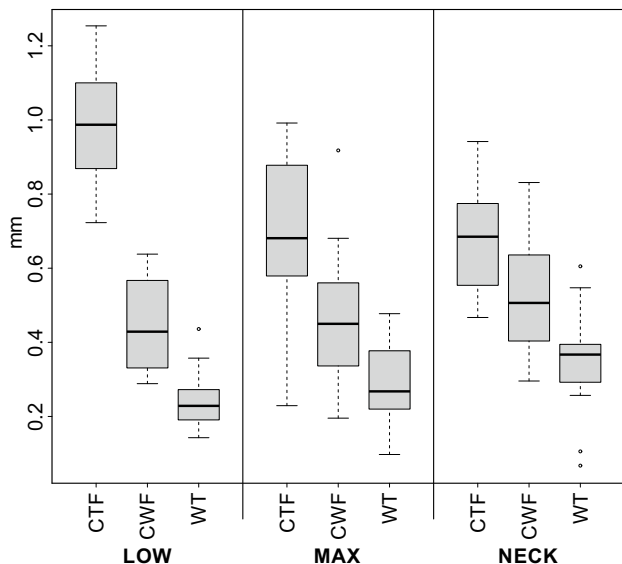
Fig. 5 Vessel regularity. 162 sections (i.e. 27 vessels × 6 sections). Distribution of the root mean square height (Rq), the rugosity parameter for the combination of section position and forming method. The distributions are ordered according to the section position

Wall thickness

In comparison with vessel regularity, mean thickness does not seem to be a good indicator of technique differentiation — the walls of the *WT* vessels are not necessarily thinner than those formed by the other techniques (Fig. 8: mean).

Nevertheless, the distributions of values for the other parameters show the same tendencies as for surface regularity — the *WT* vessels are the most standardised, followed by the vessels formed by *CWF* and, finally, the vessels formed by *CTF* (Fig. 8; Tables 6 and 7).

There is minimal variation in vessel thickness. There is almost no variation among the *WT* vessels. The values for the other two techniques vary within a range of only a few millimetres, despite the size of the vessels, and the fact that slight irregularities due to clay texture could be present. The potter has therefore succeeded in forming vessels that are highly regular in thickness.

The most clearly different sections are again from the lower parts of the vessels (Fig. 9). However, we consider this to be a preliminary observation because of the small sample size (81 sections corresponding to 9 groups). A more detailed investigation of the relationship between wall thickness and section position is required for clear conclusions to be drawn.

The variation in vessel thickness analysis performed on segments of decreasing arc length (i.e. halves, quarters and eighths) was also focused on the position showing the highest potential for forming method discrimination: the lower parts of the vessels. The similar trend as that for the *Rq* values has been observed. The differences between forming techniques decrease as the sizes of the fragments decrease (Fig. 10). However, there is almost no overlap between forming techniques even for an eighth of the arc lengths and the differences are statistically significant (Tables 8 and 9).

Table 3 Vessel surface regularity. Combination of the three section positions and three types of forming techniques. Vessel sections having the same position are highlighted by double-line boxes. Post hoc pairwise comparison using the Wilcoxon rank sum test with the Bonferroni correction

	LOW_CTF	LOW_CWF	LOW_WT	MAX_CTF	MAX_CWF	MAX_WT	NECK_CTF	NECK_CWF	NECK_WT
LOW_CTF	-								
LOW_CWF	0.00	-							
LOW_WT	0.00	0.00	-						
MAX_CTF	0.00	0.01	0.04	-					
MAX_CWF	0.00	1.00	0.00	0.04	-				
MAX_WT	0.00	0.02	1.00	0.00	0.03	-			
NECK_CTF	0.00	0.00	0.00	1.00	0.01	0.00	-		
NECK_CWF	0.00	1.00	0.00	0.42	1.00	0.00	0.28	-	
NECK_WT	0.00	1.00	0.04	0.00	1.00	1.00	0.00	0.05	-

Fig. 6 Vessel regularity. 162 sections (i.e. 27 vessels × 6 sections). Distribution of the root mean square height (Rq), the rugosity parameter for combination of section position and forming method. The distributions are ordered according to the forming method
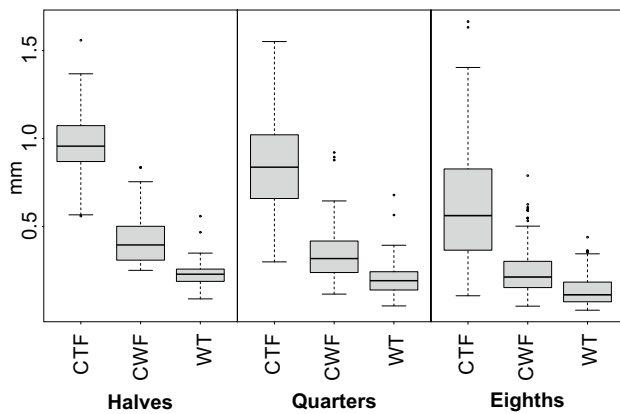
Fig. 7 Vessel regularity for the lower section. Halves = 108, quarters = 216 and eighths = 432 fragments (i.e. 27 vessels × 2 sections). Distribution of the Rq rugosity parameter according to the forming method

Table 4 Vessel surface regularity (Rq parameter) for its lower parts. Kruskal-Wallis rank sum test

	KW test	Df	p
Rq, halves ($N = 108$)	86.81	2	$< 2e{-}16$
Rq, quarters ($N = 216$)	142.09	2	$< 2e{-}16$
Rq, eighths ($N = 432$)	244.33	2	$< 2e{-}16$

Discrimination using geometric morphometrics

The results of morphometric-based discrimination calculated on all the sections show a relatively poor classification performance — only 78% of the sections were classified correctly into their original classes (Table 10). The confusion matrix reveals that, although sections of the *WT* vessels were well classified in almost all cases, the sections from the *CWF* vessels were often classified as *CTF* and vice versa (Table 11). The automatic classification was then performed separately (i) on the neck sections, (ii) on the maximum body diameter sections and (iii) on the lower part sections. Although it was possible to classify necks correctly in only 75% of cases, the classification model attained 88% for maximum body diameter sections and 96% for lower part sections (Table 12).

The confusion matrices for each part of the vessel revealed that the *WT* sections were well classified in all cases, no matter which part of the vessel was examined, while the *CTF* was well classified except for the neck sections, and the *CWF* were well-differentiated only for the lower part sections (Table 13).

Discussion

Analysis of variations in the surface roughness and the wall thickness variation shows that, with increasing contribution of rotational movement while forming, a gradual increase in vessel shape regularity and decrease in the wall thickness variability are observed. The differences in these two parameters allow us to distinguish among the studied forming methods. The initial analysis was performed on the entire horizontal section, assuming that the entire vessel was preserved. The analysis of segments of decreasing arc length also demonstrates the applicability of this approach to fragmentary archaeological pottery. The differentiation is better when larger vessel parts are preserved. However, even when only 1/8 of the horizontal section of the vessel is preserved, the forming methods are significantly different for both surface regularity and wall thickness (Tables 4, 5, 8 and 9; Figs. 7 and 10).

The automatic classification showed lower accuracy for the neck sections than for the other parts (Table 12). This was also confirmed by comparing the results of analysis of the regularity (Fig. 5) and wall thickness variability (Fig. 9) in different section positions, which show that the differences in the lower part of the vessels are the most obvious. The vessel regularity increases from the bottom parts toward the upper parts for *coiling with turntable finishing* (*CTF*) and decreases slightly for *coiling with potter's wheel finishing* (*CWF*) and *wheel-throwing* (*WT*) (Fig. 6). The hypothetical explanation for these observations is that the more complex

Table 5 Vessel surface regularity (*Rq* parameter) for its lower parts. Post hoc pairwise comparison using the Wilcoxon rank sum test with the Bonferroni correction

Rq, halves (N=108)	CTF	CWT	WT
CTF			
CWT	< 2e-16		
WT	< 2e-16	1.3e-11	

Rq, quarters (N=216)	CTF	CWT	WT
CTF			
CWT	< 2e-16		
WT	< 2e-16	9.5e-10	

Rq, eighths (N=432)	CTF	CWT	WT
CTF			
CWT	< 2e-16		
WT	< 2e-16	1.4e-15	
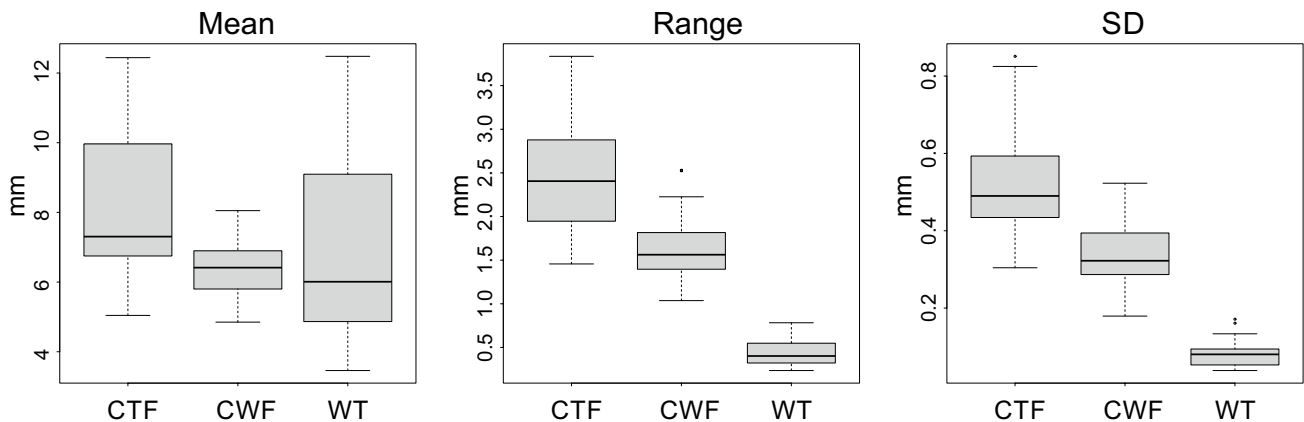
Fig. 8 Vessel wall thickness. 81 sections (i.e. 27 vessels × 3 sections). The distribution of the mean, range and standard deviation (*SD*) values for the type of forming method

Table 6 Vessel wall thickness. Kruskal-Wallis rank sum test

	KW test	Df	*p*
Mean	11.951	2	0.002541
Range	62.918	2	2.176e−14
SD	63.722	2	1.456e−14

neck shape prevents the efficient use of continuous pressure to regularise wall thickness (for the *CWF* and *WT* methods). On the other hand, the potter pays more attention to the bowl's upper body than to the lower parts. The bowl has a more complicated shape in this part, and it is also a crucial part for the overall visual impression of the vessel. Consequently, the potter spent more time fashioning the shape of the upper body of the bowl. This resulted in a more regular surface of the upper body for the forming methods, which naturally tends to produce less regular surfaces (*CTF*).

The potters' perception of the forming methods, their components and how they affect the resulting geometry are essential for insight into aspects connected with this approach. As was initially defined, *CTF* was performed only by pressure exerted by the fingers, while a potter's blade was used for *CWF*. When performing the *CTF* method, the potter felt an intense need to use the potter's blade on all parts of the vessel, and he stated that the absence of the potter's blade affected the accuracy of the vessels much more significantly than the type of rotational device (turntable vs potter's wheel). These particular observations point to the constraints of this approach. There is no simple set of basic forming methods with unambiguous implications for the geometric accuracy of the vessels. The resulting number of deviations from the ideal form depends not only on the forming method, but also more significantly on the potter's effort to produce a shape without surface irregularities. Theoretically, the particular forming methods have no significant

Table 7 Vessel wall thickness. Post hoc pairwise comparison using the Wilcoxon rank sum test with the Bonferroni correction

Mean	CTF	CWF	WT
CTF	-		
CWF	0.00089	-	
WT	0.04159	1.00000	-

Range	CTF	CWF	WT
CTF	-		
CWF	2.4e-06	-	
WT	3.1e-15	3.1e-15	-

SD	CTF	CWF	WT
CTF	-		
CWF	6.6e-07	-	
WT	3.1e-15	3.1e-15	-
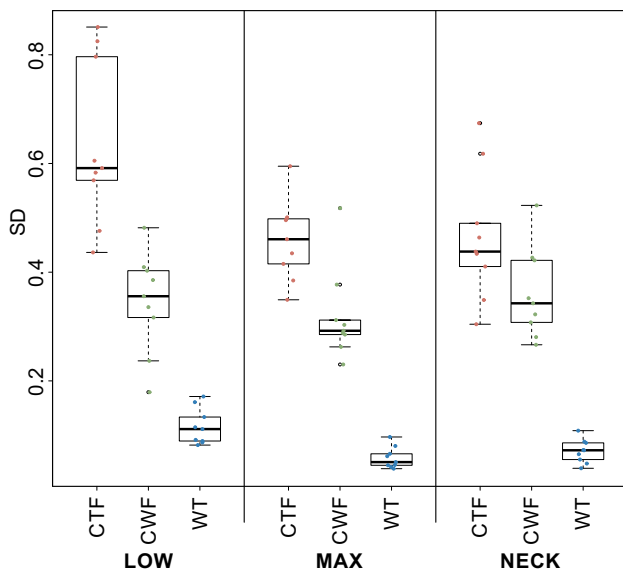
**Fig. 9** Vessel wall thickness. 81 sections (i.e. 27 vessels × 3 sections). Distribution of the standard deviation (*SD*) for the combination of forming method and section position. The distributions are ordered by section position. Data points are also shown because of the small number of samples
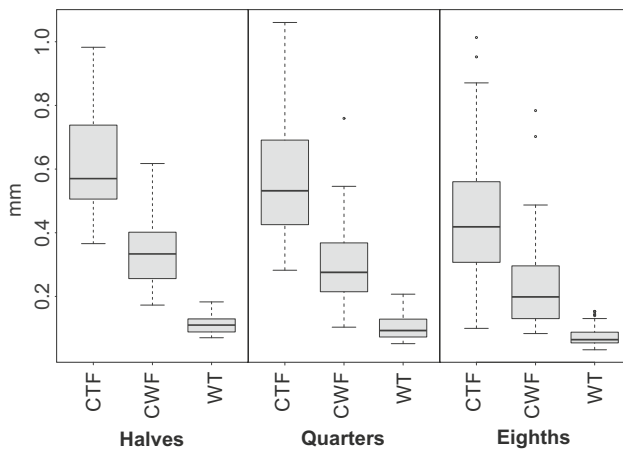
Fig. 10 Vessel wall thickness for the lower section. Halves = 54, quarters = 108 and eighths = 216 fragments (i.e. 27 vessels × 1 section). Distribution of the standard deviation (*SD*) according to the forming method

Table 8 Vessel wall thickness (*SD* parameter) for its lower parts. Kruskal-Wallis rank sum test

	KW test	Df	*p*
SD, halves (*N* = 54)	43.71	2	3.225e−10
SD, quarters (*N* = 108)	81.81	2	< 2e−16
SD, eighths (*N* = 216)	156.00	2	< 2e−16

limitations concerning the final geometric accuracy of the formed objects. The geometric and dimensional accuracy levels are mainly subject to the potter's decisions, possibilities, abilities or habits. The geometric accuracy, dimensional deviations and quality of the pottery surface would be influenced more by the social perception of aesthetics and functionality or social demand and status of the vessel than the employed forming method.

Consequently, by using any of the considered forming methods, potters can theoretically achieve an ideal shape if the forming forces act for a sufficiently long time. The difference is in the amount of work required. This problem is encountered when assigning the task to the potter. He asked how much work he should devote to each phase of the forming sequence. We agreed that he would find a reasonable balance on his own, in which he would feel that, on the one hand, the work is not performed poorly but, on the other hand, a disproportionate amount of time is not devoted to the task. The feeling-based decision represents a variable that is not entirely under control and complicates the reproducibility of the results. Even if we could define such an amount of work, we are still limited in the interpretation of the archaeological record as it is hard to separate the effect of the forming method and the effect of the amount of work dedicated to the task. The focus of the topographical analysis should reflect these aspects.

1. First of all, it is essential to focus not only on the degree of deviations from regularity but also on the geometrical character of the irregularities. They can be specific irrespective of the amount of work dedicated to obliterating them, unless wholly obliterated.
2. So far, we have discussed the limits of the forming methods in attaining geometric accuracy. However, more importantly, the forming methods are limited in their ability to "achieve" or create specific vessel irregularities. For example, using *WT*, it is not possible to "achieve" such a degree of local variability in wall thickness or deviations from the ideal form in the specific sections (cut in the plane parallel to the resulted vector of the force applied in the deformation of clay) as with, e.g. coiling or slab building. Consequently, considering our dataset, if we find that the surface regularity reaches values typical for *WT*, this does not mean that other methods can be excluded. On the other hand, if the deviations from regularity are significantly greater than that typical for *WT*, then this method can be excluded from the possible forming methods because it is impossible to obtain such irregularities when *WT* is employed. Thus, the interpretation should be based on the lower limits of regularity for wheel throwing rather than the upper limits for other methods.

🖄 Springer

Table 9 Vessel wall thickness (*SD* parameter) for its lower parts. Post hoc pairwise comparison using the Wilcoxon rank sum test with the Bonferroni correction

SD, halves (N=54)	CTF	CWT	WT
CTF			
CWT	3.8e-06		
WT	6.6e-10	2.6e-09	

SD, quarters (N=108)	CTF	CWT	WT
CTF			
CWT	4.0e-09		
WT	< 2e-16	7.3e-15	

SD, eighths (N=216)	CTF	CWT	WT
CTF			
CWT	1.9e-12		
WT	< 2e-16	< 2e-16	

Table 10 Automatic classification based on the shape of the section

Sections	Number of samples	Number of harmonics	Mean accuracy	*SD* accuracy
All sections	162	24	0.778	0.011

Table 11 Confusion matrix between 162 original forming techniques and forming techniques obtained with SVD classification run 1000 times. The values correspond to the mean value and the values in parentheses correspond to the standard deviation calculated from 1000 values. Correct correspondences are highlighted in bold. Note that the standard deviation calculation is no longer correct for very low values, close to 0. See also Table 10

All sections		Predicted		
		CTF	CWF	WT
Original	CTF	**41.7** (0.6)	12.3 (0.6)	
	CWF	16.6 (1.2)	**31.3** (1.6)	6.2 (1.2)
	WT		1.0 (0.1)	**53.0** (0.1)

Table 12 Automatic classification based on the shape of the section

Sections	Number of samples	Number of harmonics	Mean accuracy	*SD* accuracy
Neck	54	19	0.746	0.028
Maximum body diameter	54	26	0.884	0.028
Lower Part	54	23	0.961	0.021

Conclusions

The results of the pilot experimental dataset analysis show a promising potential for quantifying another phenomenon related to pottery forming: the topography and wall-thickness variation. As predicted, with the increasing contribution of rotational movement while forming, a gradual increase in the regularity of the vessel shapes and decrease in wall thickness variability is observed. The differences in these two parameters allow us to distinguish among the studied

Table 13 Three confusion matrices. Confusion matrix between 60 original forming techniques and forming techniques obtained with SVD classification. SVD run 1000 times. The values correspond to the mean value; the values in parentheses correspond to the standard deviation calculated from 1000 values. Correct correspondences are highlighted in bold. Note that the standard deviation calculation is no longer correct for very low values, close to 0. See also Table 12.

Neck		Predicted		
		CTF	CWF	WT
Original	CTF	**12.8** (1.3)	5.2 (1.3)	
	CWF	7.6 (0.6)	**9.5** (0.8)	0.9 (0.5)
	WT			**18.0** (0.1)

Maximum body diameter		Predicted		
		CTF	CWF	WT
Original	CTF	**17.9** (0.3)	0.1 (0.3)	
	CWF	3.5 (1.1)	**11.9** (1.5)	2.6 (1.0)
	WT			**18.0** (0.0)

Lower part		Predicted		
		CTF	CWF	WT
Original	CTF	**17.5** (0.5)	0.5 (0.5)	
	CWF	0.4 (0.6)	**16.4** (1.0)	1.2 (0.8)
	WT			**18.0** (0.0)

forming methods performed in the particular set of variables implemented in the experiment. All the three basic roughness parameters as a measure of deviation from the ideal form, mean height (*Ra*), maximum height (*Rz*) and root mean square height (*Rq*), show similar results. The second analysis based on comparison of the vessel thickness, calculated from the distances between points on the inner side of the vessels and their projections on the exterior, was also expressed in three measurements (the mean distance, the range of value and the standard deviation). The mean thickness does not seem to be a good indicator for identifying the forming method compared to the other two quantities. The range of values and standard deviation shows the same tendencies as the roughness measurements — the most uniform wall thickness is exhibited by *wheel-thrown* (*WT*) vessels, followed by *coiling with potter's wheel finishing* (*CWF*) and then *coiling with turntable finishing* (*CTF*). The best results are shown by the analysis of the sections obtained from the lower parts of the vessels.

However, the direct applicability of this analysis is complicated. The residual shape irregularities are substantially dependent on the potter's effort to produce a shape without irregularities. Most of the forming techniques have no significant limitations concerning the final geometric accuracy of the formed objects, at least in theory. Therefore, it is necessary to interpret the results critically with regard to all the factors that may affect the final vessel shape.

Despite these limitations, the method can objectively point out the differences in the production process and style of individual pottery traditions and become a valuable enrichment of the analysis of pottery-forming methods complementing other analytical approaches. Its applicability to fragmented archaeological pottery has been also demonstrated.

Declarations

Competing interests The authors declare no competing interests.

References

Artec 3D (2020) Space Spider. URL: https://cdn.artec3d.com/pdf/Artec3D-SpaceSpider.pdf. Accessed: 21 May 2021

Artec 3D (2021) Artec Studio 15 user guide. URL: http://docs.artec-group.com/as/15/en/_downloads/25ad86ff3ec13dc8eae3208423c3eb81/Manual-15-EN.pdf. Accessed: 21 May 2021

Berg I (2007) Meaning in the making: the potter's wheel at Phylakopi, Melos (Greece). J Anthropol Archaeol 26(2):234–252. https://doi.org/10.1016/j.jaa.2006.10.001

Berg I (2008) Looking through pots: recent advances in ceramics X-radiography. J Archaeol Sci 35(5):1177–1188. https://doi.org/10.1016/j.jas.2007.08.006

Brande S, Saragusti I (1996) A morphometric model and landmark analysis of acheulian hand axes from Norhern Israel. In: Marcus LF, Corti M, Loy A, Naylor GJP, Slice DE (eds) Advances in Morphometrics. Plenum Press, pp. 423-435

Brown CT, Witschey WRT, Liebovitch LS (2005) The broken past: fractals in archaeology. J Archaeol Method Theory 12(1):37–78. https://doi.org/10.1007/s10816-005-2396-6

Buchanan B, Collard M (2010) A geometric morphometrics-based assessment of blade shape differences among Paleoindian projectile point types from western North America. J Archaeol Sci 37(2):350–359. https://doi.org/10.1016/j.jas.2009.09.047

Chernov N (2010) Circular and linear regression: fitting circles and lines by least squares. CRC Press

Choleva M (2012) The first wheelmade pottery at Lerna: wheel-thrown or wheel-fashioned? Hesperia J Am Schl Class Stud Athens 81(3):343–381. https://doi.org/10.2972/hesperia.81.3.0343

Cortes C, Vapnik V (1995) Support-vector networks. Mach Learn 20(3):273–297. https://doi.org/10.1007/BF00994018

Courty MA, Roux V (1995) Identification of wheel throwing on the basis of ceramic surface features and microfabrics. J Archaeol Sci 22(1):17–50. https://doi.org/10.1016/S0305-4403(95)80161-8

Derenne E, Ard V, Besse M (2020) Pottery technology as a revealer of cultural and symbolic shifts: funerary and ritual practices in the Sion 'Petit-Chasseur' megalithic necropolis (3100–1600 BC, Western Switzerland). J Anthropol Archaeol 58:101170. https://doi.org/10.1016/j.jaa.2020.101170

Doherty SK (2015) Origins and use of the potter's wheel in ancient Egypt. Archaeopress.

Dupont-Delaleuf A (2011) Styles techniques des céramiques de la protohistoire en Asie Centrale: méthodologie et études de cas (Ph.D. thesis). Université Paris Ouest La Défense

Evans AA, Donahue RE (2008) Laser scanning confocal microscopy: a potential technique for the study of lithic microwear. J Archaeol Sci 35(8):2223–2230. https://doi.org/10.1016/j.jas.2008.02.006

Evans AA, Macdonald D (2011) Using metrology in early prehistoric stone tool research: further work and a brief instrument comparison. Scanning 33(5):294–303. https://doi.org/10.1002/sca.20272

Evans AA, Lerner H, Macdonald DA, Stemp WJ, Anderson PC (2014) Standardization, calibration and innovation: a special issue on lithic microwear method. J Archaeol Sci 48:1–4. https://doi.org/10.1016/j.jas.2014.03.002

Faulks NR, Kimball LR, Hidjrati N, Coffey TS (2011) Atomic force microscopy of microwear traces on Mousterian tools from Myshtylagty Lagat (Weasel Cave), Russia. Scanning 33(5):304–315. https://doi.org/10.1002/sca.20273

Furuta N, Ninomiya S, Takahashi N, Ohmori H, Ukai Y (1995) Quantitative evaluation of soybean (Glycine max L. Merr.) leaflet shape by principal component scores based on elliptic fourier descriptor. Breed Sci 45(315–320)

Gallay A (2012) Potières du Sahel: à la découverte des traditions céramiques de la boucle du Niger (Mali). Infolio

Gelbert A (2003) Traditions céramiques et emprunts techniques dans la vallée du fleuve Sénégal. Maison des sciences de l'homme : Epistèmes

Gomart L (2011) Pottery traditions and manufacturing organization in the early neolithic: a method for the technological study of Linearbandkeramik vases in habitat contexts in the Aisne Valley (France). Sprawozdania Archeologiczne 63:189–201

Gomart L (2014) Traditions techniques & production céramique au Néolithique ancien: étude de huit sites rubanés du nord est de la France et de Belgique. Sidestone Press

Gomart L, Constantin C, Burnez-Lanotte L (2017) Ceramic production and village communities during the Early Neolithic in north-eastern France and Belgium. Issues regarding tempers and pot-forming processes. In: Burnez-Lanotte L (ed) Matières à Penser: Sélection et Traitement Des Matières Premières Dans Les Productions Potières Du Néolithique Ancien. Société préhistorique française, pp 133–156

Gosselain OP (1998) Social and technical identity in a clay crystal ball. In: Stark MT (ed) The archaeology of social boundaries. Smithsonian Institution Press, pp 78–106

Gosselain OP (2000) Materializing identities: an African perspective. J Archaeol Method Theory 7(3):187–217. https://doi.org/10.1023/A:1026558503986

Gosselain OP (2002) Poteries du Cameroun méridional: styles techniques et rapports à l'identité. CNRS éditions

Gosselain OP (2008) Mother Bella was not a Bella: inherited and transformed traditions in Southwestern Niger. In: Stark MT, Bowsler BJ, Horne L (eds) Cultural transmission and material culture: breaking down boundaries. University of Arizona Press, pp 150–177

Halíř R (1999) An automatic estimation of the axis of rotation of fragments of archaeological pottery: a multi-step model-based approach. In Skala V (ed) 7-th International Conference in Central Europe on Computer Graphics, Visualization and Interactive Digital Media'99 (WSCG'99)

Henrickson RC (1991) Wheelmade or wheel-finished? Interpretation of 'wheelmarks' on pottery. In: Druzik JR, Vandiver PB, Wheeler G (eds) Materials issues in art and archaeology II. Materials Research Society, pp 523–541

Hodson FR, Sneath PHA, Doran JE (1966) Some experiments in the numerical analysis of archaeological data. Biometrika 53(3–4):311–324. https://doi.org/10.1093/biomet/53.3-4.311

ISO (2012) ISO 25178-2:2012 Geometrical product specifications (GPS) — surface texture: areal — part 2: terms, definitions and surface texture parameters. URL: https://www.iso.org/standard/42785.html

Jeffra CD (2013) A re-examination of early wheel potting in Crete. Annu Br Schl Athens 108:31–49. https://doi.org/10.1017/S0068245413000038

Karasik A, Smilansky U (2008) 3D scanning technology as a standard archaeological tool for pottery analysis: practice and theory. J Archaeol Sci 35(5):1148–1168. https://doi.org/10.1016/j.jas.2007.08.008

Key AJM, Stemp WJ, Morozov M, Proffitt T, de la Torre I (2015) Is Loading a significantly influential factor in the development of lithic microwear? An experimental test using LSCM on basalt from Olduvai Gorge. J Archaeol Method Theory 22(4):1193–1214. https://doi.org/10.1007/s10816-014-9224-9

Kimball LR, Kimball JF, Allen PE (1995) Microwear polishes as viewed through the atomic force microsope. Lithic Technol 20(1):6–28

Knappett C (1999) Tradition and innovation in pottery forming technology: wheel-throwing at Middle Minoan Knossos. Annu Br Schl Athens 94:101–129

Kudelić A (2020) Trace evidence of pottery forming techniques: early Urnfield culture vessels. In: Miloglav I (ed) Recent developments in archaeometry and archaeological methodology in South-eastern Europe. Cambridge Scholars Publishing, pp 58–81

Kuhl FP, Giardina GR (1982) Elliptic Fourier features of a closed contour. Comput Graph Image Process 18:236–258

Laskaris N, Liritzis I, Bonini M, Ridi F, Kersting R, Al-Otaibi F (2017) AFM and SIMS surface and cation profile investigation of archaeological obsidians: new data. J Cult Herit 25:101–112. https://doi.org/10.1016/j.culher.2016.11.014

Lestrel PE (1997) Introduction and overview of Fourier descriptors. In: Lestrel PE (ed) Fourier descriptors and their applications in biology. Combridge University Press, pp 22–44

Macdonald DA (2014a) The application of focus variation microscopy for lithic use-wear quantification. J Archaeol Sci 48:26–33. https://doi.org/10.1016/j.jas.2013.10.003

Macdonald DA (2014b) The application of focus variation microscopy for lithic use-wear quantification. Lithic Microwear Method Standard Calibr Innov 48:26–33. https://doi.org/10.1016/j.jas.2013.10.003

Macdonald DA, Evans AA (2014) Evaluating surface cleaning techniques of stone tools using laser scanning confocal microscopy. Microsc Today 22(3):22–27. https://doi.org/10.1017/S1551929514000364

Macdonald DA, Harman R, Evans AA (2018) Replicating surface texture: preliminary testing of molding compound accuracy for surface measurements. J Archaeol Sci Rep 18:839–846. https://doi.org/10.1016/j.jasrep.2018.02.033

Martineau R (2002) Poterie, techniques et sociétés. Etudes analytiques et expérimentales à Chalain et Clairvaux (Jura), entre 3200 et 2900 av.J.-C. Bulletin de la Société préhistorique française 99(1):150–153

Mayor A (2010) Ceramic traditions and ethnicity in the Niger Bend, West Africa. Ethnoarchaeology 2(1):5–48. https://doi.org/10.1179/eth.2010.2.1.5

Méry S, Dupont-Delaleuf A, van der Leeuw SE (2012) Les techniques de façonnage céramique mettant en jeu la rotation à Hili (Émirats arabes unis) à la fin du IIIe millénaire (âge du Bronze ancien). Nouvelles de l'Archéologie 119:52–64

Moropoulou A, Delegou ET, Vlahakis V, Karaviti E (2007) Digital processing of SEM images for the assessment of evaluation indexes of cleaning interventions on Pentelic marble surfaces. Mater Charact 58(11–12):1063–1069. https://doi.org/10.1016/j.matchar.2007.04.021

O'Connor J, Sexton B, Smart RSC (eds) (2003) Surface analysis methods in materials science, 2nd edn. Springer-Verlag. https://doi.org/10.1007/978-3-662-05227-3

Revello Lami, M., Opgenhaffen, L., & Kisjes, I. (2016). Pottery goes digital: 3D laser scanning technology and the study of archaeological ceramics. In S. Campana, R. Scopigno, G. Carpentiero, & M. Cirillo (Eds.), CAA2015: Keep the revolution going: proceedings of the 43rd annual conference on computer applications and quantitative methods in archaeology (vol. 1, pp. 421–431). Archaeopress Publishing

Rice PM (2015) Pottery analysis: a sourcebook, 2nd edn. University of Chicago Press

Rohlf F, Archie J (1984) A comparison of Fourier methods for the description of wing shape in mosquitoes (Diptera: Culicidae). Syst Zool 33(3):302–317

Rosselló JG, Trias MC (2013) Making pots: el modelado de la cerámica a mano y su potencial interpretativo. Archaeopress

Roux V (2003) A dynamic systems framework for studying technological change: application to the emergence of the potter's wheel in the southern Levant. J Archaeol Method Theory 10(1):1–30. https://doi.org/10.1023/A:1022869912427

Roux V (2011) Anthropological interpretation of ceramic assemblages: foundations and implementations of technological analysis. In: Scarcella S (ed) Archaeological ceramics: a review of current research. Archaeopress, pp 80–88

Roux V (2017) Ceramic manufacture: the chaîne opératoire approach. In: Hunt AMW (ed) The Oxford handbook of archaeological ceramic analysis. Oxford University Press, pp 101–114

Roux V (2019) Ceramics and society: a technological approach to archaeological assemblages. Springer. https://doi.org/10.1007/978-3-030-03973-8

Roux V, Courty MA (1998) Identification of wheel-fashioning methods: technological analysis of 4th-3rd millennium oriental ceramics. J Archaeol Sci 25(8):747–763. https://doi.org/10.1006/jasc.1997.0219

Roux V, Bril B, Cauliez J, Goujon A-L, Lara C, Manen C et al (2017) Persisting technological boundaries: social interactions, cognitive correlations and polarization. J Anthropol Archaeol 48:320–335. https://doi.org/10.1016/j.jaa.2017.09.004

Rückl Š, Jacobs L (2016) "With a little help from my wheel": wheel-coiled pottery in Protogeometric Greece. Hesperia: J Am Schl Class Stud Athens 85(2):297–321. https://doi.org/10.2972/hesperia.85.2.0297

Rye OS (1981) Pottery technology: principles and reconstruction. Taraxacum

Sablatnig R, Mara H, Kampel M (2005) Estimation of rotational symmetry based on concentric circular rills. Presented at the Joint Hungarian-Austrian Conference on Image Processing and Pattern Recognition, Proc. of the 29th Workshop of the Austrian Association for Pattern Recognition (OAGM/AAPR); 01/2005

Sahoo P (2011) Surface topography. In: Davim JP (ed) Tribology for engineers, vol 1. Woodhead Publishing, pp 1–32. https://doi.org/10.1533/9780857091444.1

Stemp WJ (2014) A review of quantification of lithic use-wear using laser profilometry: a method based on metrology and fractal analysis. J Archaeol Sci 48:15–25

Stemp WJ, Stemp M (2001) UBM laser profilometry and lithic use-wear analysis: a variable length scale investigation of surface topography. J Archaeol Sci 28(1):81–88. https://doi.org/10.1006/jasc.2000.0547

Stemp WJ, Stemp M (2003) Documenting stages of polish development on experimental stone tools: surface characterization by fractal geometry using UBM laser profilometry. J Archaeol Sci 30:287–296

Stemp WJ, Childs BE, Vionnet S, Brown CA (2008) The quantification of microwear on chipped stone tools: assessing the effectiveness of root mean square roughness (Rq). Lithic Technol 33(2):173–189. https://doi.org/10.1080/01977261.2008.11721067

Stemp WJ, Childs BE, Vionnet S, Brown CA (2009) Quantification and discrimination of lithic use-wear: surface profile measurements and length-scale fractal analysis. Archaeometry 51(3):366–382. https://doi.org/10.1111/j.1475-4754.2008.00404.x

Stemp WJ, Childs BE, Vionnet S (2010) Laser profilometry and length-scale analysis of stone tools: second series experiment results. Scanning 32(4):233–243. https://doi.org/10.1002/sca.20200

Stemp WJ, Lerner HJ, Kristant EH (2013) Quantifying microwear on experimental mistassini quartzite scrapers: preliminary results of exploratory research using LSCM and scale-sensitive fractal analysis: quantifying microwear on experimental Mistassini quartzite scrapers. Scanning 35(1):28–39. https://doi.org/10.1002/sca.21032

Stemp WJ, Watson AS, Evans AA (2015a) Surface analysis of stone and bone tools. Surf Topogr Metrol Prop 4(1):013001. https://doi.org/10.1088/2051-672X/4/1/013001

Stemp WJ, Morozov M, Key AJM (2015b) Quantifying lithic microwear with load variation on experimental basalt flakes using LSCM and area-scale fractal complexity (Asfc). Surf Topogr Metrol Prop 3(3):034006. https://doi.org/10.1088/2051-672X/3/3/034006

Thér R (2016) Identification of pottery-forming techniques using quantitative analysis of the orientation of inclusions and voids in thin sections. Archaeometry 58(2):222–238. https://doi.org/10.1111/arcm.12166

Thér R (2020) Ceramic technology. How to reconstruct and describe pottery-forming practices. Archaeol Anthropol Sci 12(8):172. https://doi.org/10.1007/s12520-020-01131-0

Thér R, Toms P (2016) Quantification of the orientation and alignment of aplastic components of a ceramic body as a method for distinguishing among various means of using a rotational device in pottery forming. J Archaeol Sci Rep 9:33–43. https://doi.org/10.1016/j.jasrep.2016.06.048

Thér R, Mangel T, Gregor M (2017) Potter's wheel in the Iron Age in Central Europe: process or product innovation? J Archaeol Method Theory 1–44. https://doi.org/10.1007/s10816-016-9312-0

van Doosselaere B (2010) Poterie et histoire au temps des grands empires ouest africains études technologiques de l'assemblage céramique de Koumbi Saleh (Mauritanie 6e - 17e siècles) (Ph.D. thesis). Université Paris 1 - Panthéon Sorbonne

Werner JJ (2018) An experimental investigation of the effects of post-depositional damage on current quantitative use-wear methods. J Archaeol Sci Rep 17:597–604. https://doi.org/10.1016/j.jasrep.2017.12.008

Whitehouse DJ (2002) Surfaces and their measurement. Hermes Penton Ltd.

Wilczek J, Monna F, Barral P, Burlet L, Chateau C, Navarro N (2014) Morphometrics of Second Iron Age ceramics - strengths, weaknesses, and comparison with traditional typology. J Archaeol Sci 50:39–50

Wilczek J, Monna F, Jébrane A, Chazal CL, Navarro N, Couette S, Smith CC (2018) Computer-assisted orientation and drawing of archaeological pottery. J Comput Cult Herit 11(4):22:1-22:17. https://doi.org/10.1145/3230672

Zhan Q-B, Wang X-L (2012) Elliptic Fourier analysis of the wing outline shape of five species of antlion (Neuroptera: Myrmeleontidae: Myrmeleontini). Zool Stud 51(3):399–405

Zorlu K (2008) Description of the weathering states of building stones by fractal geometry and fuzzy inference system in the Olba ancient city (Southern Turkey). Eng Geol 101(3–4):124–133. https://doi.org/10.1016/j.enggeo.2008.04.005

Springer